

pubs.acs.org/acschemicalbiology Article

Synthesis and Biophysical Properties of 3'-Deoxy- β -D-apio-D-furanosyl Nucleic Acids

Victorio Jauregui-Matos, Dhrubajyoti Datta, Jayanta Kundu, Vathan Kumar, Joel M. Harp, Adekunle Adebayo, Daniel Donnelly, Esau Medina, John C. Chaput, Martin Egli, and Muthiah Manoharan*



Cite This: https://doi.org/10.1021/acschembio.5c00591



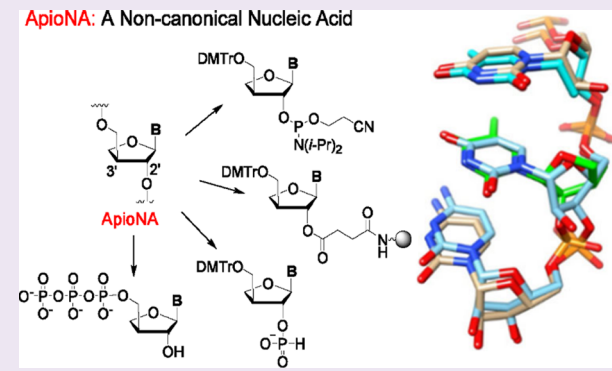
ACCESS

III Metrics & More

Article Recommendations

Supporting Information

ABSTRACT: Inspired by the uncommon furanose configuration of 3'-deoxyapio-containing nucleic acids (apioNAs), we developed a facile and convenient synthesis of 24 building blocks of this modified nucleic acid monomer, including phosphoramidites, *H*-phosphonates, solid supports, and nucleoside triphosphates. The building blocks included those containing the four canonical RNA bases A, G, U, and C as well as T and 5-methyl-C and were synthesized starting from a single common sugar intermediate derived from D-(+)-xylose. DNA and RNA duplexes with a single apioNA modification in one strand were less thermodynamically stable than unmodified DNA or RNA. The crystal structure of apioNA-modified RNA octamer showed that the apioNA residue adopts an RNA-like structure but local reorientation of the apioNA sugar and 2'-phosphate and the difference in helical rise on the



5' side of the apioNA T relative to RNA likely contribute to the destabilizing effect of apioNA residues. At the terminus of a DNA strand, this modification provides extremely high resistance against both 3'- and 5'-exonucleases even when linked to the adjacent residue by a phosphodiester moiety. Molecular modeling of a DNA duplex containing apioNA was used to rationalize the DNA duplex destabilization and the exonuclease resistance resulting from incorporation of the apioNA residue. Use of apioNA NTPs as substrates for previously engineered α -L-threofuranosyl polymerases depends on both the enzyme and the nucleobase. These data indicate that apioNAs warrant further evaluation, and the building blocks synthesized will allow incorporation of apioNA into therapeutic oligonucleotides.

■ INTRODUCTION

In 1901, apiose was shown to be a sugar component in parsley and a cell wall stabilizer in aquatic monocots. 1,2 This unique branched-chain pentose is now the basis for antivirals, lymphocyte inhibitors, and anticancer agents.3-10 Both Dand L-apio nucleoside analogues with 2' hydroxyl groups have potential as anti-HIV agents. 11 Apiose has been synthesized from xenobiotic sugar precursors, and it has been incorporated into nucleotide triphosphates by enzymatic catalysis. 3,12-17 3'-Deoxy- β -D-apio-D-furanosyl nucleosides (apioNAs) have a structure similar to that of α -L-threofuranosyl nucleosides (TNAs) (Figure 1). TNA, due to its resistance to endo- and exonucleases and acid-mediated degradation 18,19 and its ability to self-pair and to cross-pair with RNA and DNA strands, ²⁰ has potential for use in nucleic acid-based therapeutics. 21-27 Polymerases have been engineered that use TNA nucleoside triphosphates (NTPs) as substrates, and this has allowed selection of aptamers, which are short oligonucleotides with high affinity to various protein and small-molecule targets, that have potential as therapeutics and diagnostic tools. 28,29

Like TNA, the apioNA backbone connects neighboring nucleotides through the 2' and 3' carbons of the pentose; however, TNA links repeating units with five covalent bonds, whereas apioNA possesses an additional methylene group emanating from the 3'-C that provides an additional bond to afford a six-bond distance between units, making it a regioisomer of 2'-deoxyribose (Figure 1A). The unusual 2'-3' connectivity of apioNA makes it an interesting candidate for applications in biomedicine. Yamada et al. and Datta et al. have shown that 6'-morpholino, 6'-piperidino, methylene-extended nucleotides, and 6'-(E)- and 6'-(Z)-vinylphosphonates, which all have extended backbones, mitigate off-target effects and enhance efficacies of small interfering RNA (siRNA) when placed at certain positions. 30-32 Given the similarities to these

Received: July 31, 2025
Revised: September 29, 2025
Accepted: September 30, 2025



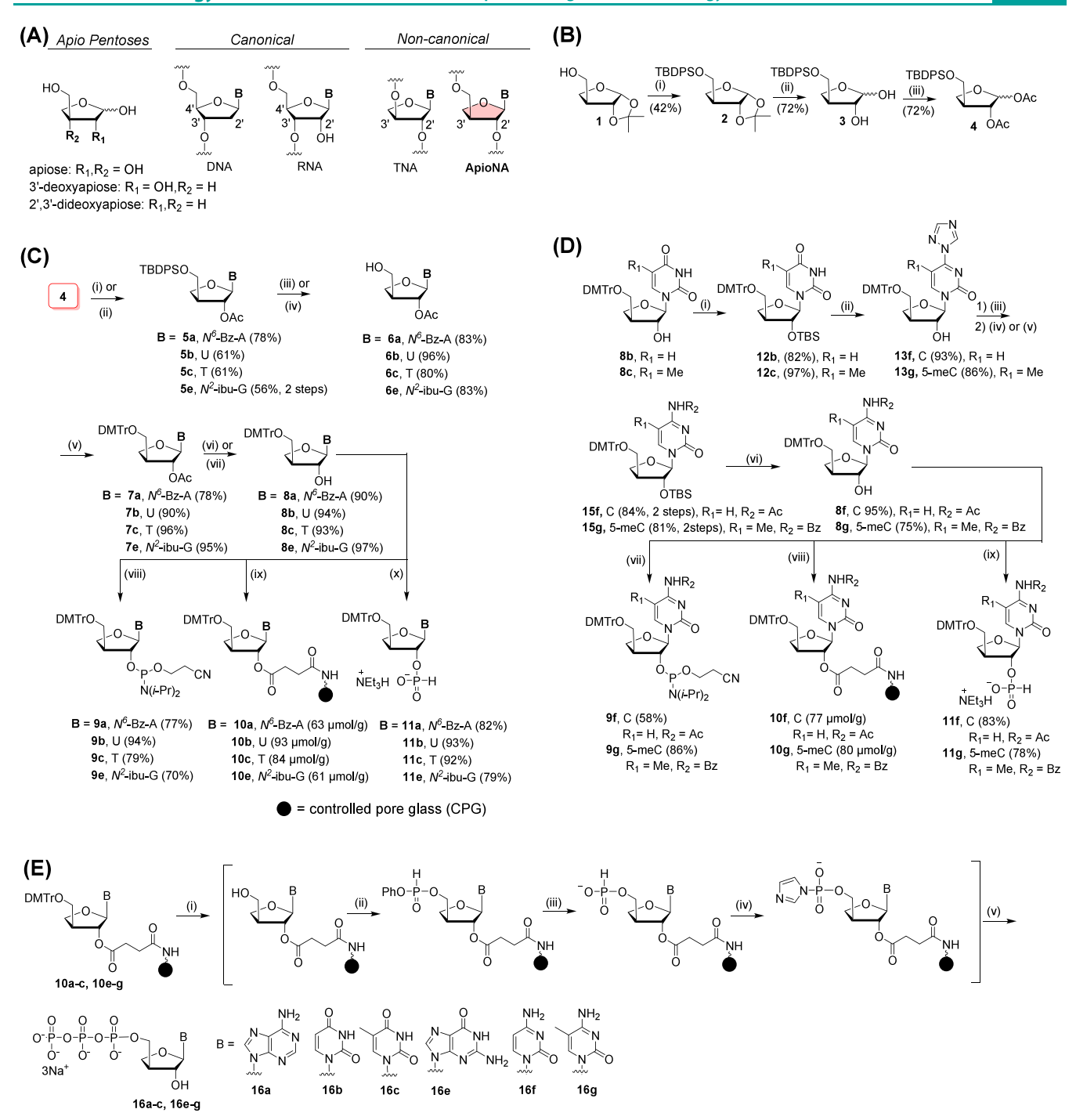


Figure 1. (A) Structures of apio pentoses and canonical and noncanonical nucleosides (where B is the nucleobase). (B) Preparation of diacetate 3'-deoxyapiose sugar 4. (C) Synthesis of U, T, N^6 -Bz-A, and N^2 -ibu-G apioNA building blocks. (D) Synthesis of N^4 -Ac-C and N^4 -Bz-5-Me-C apioNA building blocks. (E) Solid-phase synthesis of apioNA triphosphates. See Scheme S2 for detailed experimental conditions for B–E.

nucleic acid analogs, apioNAs warrant further investigation, and we undertook the synthesis of apioNA building blocks with the goal of testing them in the context of therapeutic oligonucleotides.

While our work was in progress, synthesis of T, C, A, and G apioNA phosphoramidites and their incorporation into oligonucleotide sequences were reported in the patent literature.^{33,34} In these procedures either the pentose sugar intermediate was a mixture, which requires separation before making nucleoside precursors,³³ or a multistep homologation of the TNA nucleoside precursor was needed.³⁴ In contrast,

our synthetic route unambiguously maintains the stereopurity of the pentose sugar, as the starting material is derived from the 1,2-*O*-isopropylidene-α-D-xylose which was derived from naturally occurring D-(+)-xylose. D-(+)-Xylose is primarily found in plant biomass, particularly in hemicellulose, a major component of wood and agricultural residues, and in smaller amounts in the embryos of many edible plants.³⁵ We synthesized apioNA building blocks bearing the four canonical RNA nucleobases A, U, G, and C as well as T and 5-methyl-C (5-meC) as phosphoramidites, *H*-phosphonates, solid supports, and nucleotide triphosphates. We evaluated binding

affinities of apioNA-substituted oligonucleotides to RNA and DNA and susceptibilities of oligonucleotides bearing apioNAs to exonuclease-mediated degradation, and the results are rationalized based on molecular modeling and a crystal structure of an apio-T modified RNA. As these nucleic acids are related to TNAs, we evaluated polymerization of apioNA NTPs by polymerases engineered to use TNAs as substrates.²⁸

■ RESULTS AND DISCUSSION

Syntheses of apioNA Building Blocks and Oligonucleotides Containing ApioNA. The acyl-protected 3'deoxyapiose sugar 4 was previously synthesized. 5,6,14 Here we report an optimized route to furnish 4 from ketal 1 synthesized as previously described⁵ (Scheme S1). The synthesis began with the naturally occurring sugar D-(+)-xylose, which after acetonide protection and deprotection afforded 1,2-O-isopropylidene-D-xylofuranose S2 in quantitative yield. Mitsunobu reaction of the primary hydroxyl group followed by azobisisobutyronitrile (AIBN)-mediated deoxygenation afforded 1,2-O-isopropylidene-D-threose (S4), which can also be prepared from L-ascorbic acid in a multistep synthesis.⁵ Further oxidation of the secondary hydroxyl group followed by the Wittig reaction afforded olefin intermediate S6, which upon hydroboration-oxidation exclusively elicited S7, the undesired α isomer. Three cycles of acid and base treatment of \$7 produced the desired intermediate 1 along with unreacted S7. Intermediate 1 was subjected to silyl protection of the primary 4'-hydroxyl using tert-butyldiphenylsilyl chloride (TBDPSCl) in the presence of imidazole to afford 2. Subsequent ketal deprotection of 2 with a 1.0 M solution of boron trichloride in dichloromethane (DCM) and n-hexanes yielded the anomeric mixture of diols 3 in a reasonable yield. Finally, acyl protection of the diols with acetic anhydride in the presence of pyridine and a catalytic amount of 4-dimethylaminopyridine (DMAP) afforded the protected 3'deoxyapiose sugar 4 suitable for glycosylation reactions under well-known conditions (Figure 1B).

The 3'-deoxyapio U, T, N2-ibu-G, and N6-Bz-A phosphoramidites were synthesized as depicted in Figure 1C. Glycosylations were performed using the silyl-Hilbert–Johnson/Vorbrüggen reaction parameters. 36,37 The general conditions included the use of N,O-bis(trimethylsilyl)acetamide (BSA) as the silylating agent, trimethylsilyl triflate (TMSOTf) as the Lewis acid, and 1,2-dichloroethane (DCE) as the solvent. The N-9 and β -exclusive glycosylation products of N^6 -Bz-A (5a) and N^2 -ibu-G (5e) were obtained at 65–70 °C, but a lower temperature of 25 °C had to be employed for the pyrimidines to achieve exclusively the desired β glycosylation products 5b and 5c in decent yields. Initially, when we used acetonitrile as the solvent, we obtained a mixture of anomeric glycosylation products. Changing the solvent from acetonitrile to DCE afforded exclusively the desired β -anomer for pyrimidine nucleosides. Desilylation of the primary alcohol with a 1.0 M solution of tetrabutylammonium fluoride (TBAF) in THF or 37% HF in triethylamine (HF·3Et₃N) afforded the desilylated nucleosides 6a-c and 6e in good yields. In the 2D NOESY NMR spectra, the 3'-OH proton of apiose sugar showed NOE interaction with HN-3 in U, BzHN-6 in A, and HN-1 and ibuNH-2 in G (Figure S1), thus confirming that the β -exclusive and desired regiosiomers were obtained in these glycosylation reactions. Subsequent tritylation with 4,4-dimethoxytrityl chloride with catalytic DMAP in anhydrous pyridine resulted in the tritylated

products 7a-c and 7e in high yields. 2'-Deacylation of the sugar with 1 M aqueous NaOH in THF/MeOH (1:1) was performed at 25 °C for U and T (8a and 8b), whereas for N^6 -Bz-A and N^2 -ibu-G (8c and 8e) the reaction was carried out at 0 °C to prevent the deprotection of the exocyclic amino groups. Lastly, phosphitylation yielded the phosphoramidites 9a-c and 9e in yields ranging from 70% to 94%.

The C and 5-meC phosphoramidites were synthesized starting from iso-5'-O-DMTr-2'-hydroxy intermediates of U and T as shown in Figure 1D. 8b and 8c were subjected to imidazole and tert-butyldimethylsilyl chloride to protect the 2'hydroxyl groups, yielding silylated alcohols 12b and 12c. Triazolylation of the oxygen at position 4 was achieved with an excess of 1,2,4-triazole and Et₃N in the presence of phosphorus oxychloride, which gave triazole derivatives 13f and 13g in 93% and 94% yield, respectively. Further displacement of the triazole group with 28% NH₄OH yielded 14g and 14f in good yields. To make the suitably protected phosphoramidites of C and 5-meC, monoacylation of N-4 was performed with acetic anhydride for C and benzoic anhydride for 5-meC to afford protected amines 15g and 15f. The 2'-O-tert-butyldimethylsilyl group was removed with 1.0 M TBAF in THF to furnish the free 2'-hydroxyl groups for phosphitylation. Lastly, phosphitylation of the 2'-hydroxyl groups gave the phosphoramidites of N^4 -Ac-C and N^4 -Bz-5-meC (9f and 9g, respectively) in good yields.

We also synthesized triethylamine salts of H-phosphonates as building blocks for P(V) chemistry. The H-phosphonate building blocks 11a-c and 11e-g were synthesized from the corresponding 3'-deoxyapioNA nucleosides in a single step in moderate to good yields (78-93%) (Figure 1C,D). Finally, we used the nucleoside building blocks to make the corresponding succinates by treating 8a-8c, 8f, and 8g with succinic anhydride under basic conditions followed by coupling to the amine-modified controlled pore glass (CPG) (Figure 1C,D). The modified CPGs thus obtained (10a-10c and 10e-10g) were used in the syntheses of 3'-modified oligonucleotides. The phosphoramidite building blocks of all synthesized apioNAs were incorporated into oligonucleotides under standard conditions (Table S1-S3). To obtain triphosphate analogs of apioNA, H-phosphonate chemistry was employed. The triphosphates 16a-c and 16e-g were synthesized on an ABI-394 DNA/RNA synthesizer using a previously described protocol³⁸ (Figure 1E and Table S7). Previously, these triphosphates were synthesized using a solution-phase method.3

ApioNA Residues Destabilize Binding Affinity of Nucleic Acid Duplexes and Behave like TNA. Oligonucleotides were synthesized to test the effects of a single apioNA residue or an apioNA base pair on RNA, DNA, and RNA/ DNA hybrid duplexes. All apioNA modifications thermally destabilized the 12-mer RNA duplex, with the thermal melting temperature $(T_{\rm m})$ reduced by 5–6 °C (Table 1). Differences in destabilization between purine and pyrimidine apioNA residues were minimal in the context of the RNA duplexes. When the apioNA-containing strand was RNA and the complementary strand was DNA, the destabilization ranged from 5 to 9 °C; again, differences between purines and pyrimidines were minimal (Table S4). When the apioNAcontaining strand was DNA and the complementary strand was RNA, the pyrimidine apioNAs were destabilizing by about 6.5 °C, whereas the purines were either slightly destabilizing (apioNA A, -1.0 °C) or slightly stabilizing (apioNA G, +0.7

Table 1. Melting Temperatures of RNA Duplexes with Single ApioNA Modifications or ApioNA Base Pairs

Oligo ID	Sequences ^a	T _m (°C)	$\Delta T_m(^{\circ}C)^b$
ON11	5'-r(UACAGUCUAUGU)-3'	52.0	NA
ON12	3'-r(AUGUCAGAUACA)-5'		
ON13	5'-r(UACAGTCUAUGU)-3'	46.0	-6.0
ON12	3'-r(AUGUCAGAUACA)-5'		
ON14	5'-r(UACAGUCUAUGU)-3'	46.3	-5.7
ON12	3'-r(AUGUCAGAUACA)-5'		
ON11	5'-r(UACAGUCUAUGU)-3'	46.5	-5.5
ON15	3'-r(AUGUCAGAUACA)-5'		
ON11	5'-r(UACAGUCUAUGU)-3'	46.0	-6.0
ON16	3'-r(AUGUCAGAUACA)-5'		
ON13	5'-r(UACAGTCUAUGU)-3'	42.2	-9.8
ON15	3'-r(AUGUCAGAUACA)-5'		
ON14	5'-r(UACAGUCUAUGU)-3'	40.2	-11.8
ON16	3'-r(AUGUCAGAUACA)-5'		

^aUppercase letters indicate RNA. Uppercase colored bold letters indicate apioNA residues. $^b\Delta T_{\rm m}$ is the difference in melting temperature between the modified duplex and the reference RNA duplex ON11/ON12.

°C) (Table S5). The apioNA modifications considerably destabilized a DNA duplex, with decreases in $T_{\rm m}$ ranging from 5.2 to 17.7 °C; the purine apioNAs were less destabilizing than the pyrimidine ones (Table S6). Additive destabilizing effects were observed for apioNA base pairs in the context of both the RNA duplex and the DNA duplex (Tables 1 and S6). An apioNA-apioNA base pair in the context of an RNA duplex was more destabilizing than a single apioNA, with a $T_{\rm m}$ reduction of 9.8 °C for a T-A apioNA base pair and 11.8 °C for a C-G base pair. Interestingly, in a similar manner, a TNA-TNA base pair in the context of an RNA duplex was also more destabilizing than a single TNA, with a T_{m} reduction of 9.5 °C for a T-A TNA base pair and 11.0 °C for a C-G base pair.²¹ The fact that apioNA is as destabilizing as TNA even with an additional -CH2-, which should provide more flexibility, is interesting. The East pucker, a ca. 10° buckle for base pairs, and the slightly increased rise with apio-T observed in the crystal structure data shown below can account for this. The additional methylene in apioNA and loss of stacking as a result could also contribute, as stacking makes the most important contribution to nucleic acid pairing stability. Even the 0.1 Å change in the stacking distance that is seen here could make quite a difference.

Crystal Structure of an ApioNA T-Modified RNA Octamer. The crystal structure of a self-complementary RNA duplex modified with apioNA T, $[5'-(Br^5C)GAAU-(apio-T)CG-3']_2$, was determined at a resolution of 1.35 Å. The asymmetric unit of the crystal with space group $P2_1$ and unit cell constants a=48.59 Å, b=39.31 Å, c=76.25 Å, and $\beta=94.7^{\circ}$ contained seven independent duplexes. The structure was refined to final values of 0.206 for R_{work} and 0.264 for R_{free} (test set 5%) using 63,133 reflections in the 28.77 to 1.35 Å resolution range with a completeness of 98.3% and rmsd values of 0.016 Å for bond lengths and 1.8° for bond angles. Data collection and refinement statistics are presented in Table S8. The structure was deposited in the Protein Data Bank with the ID code 9Q3C.

All apioNA T residues adopt the O4'-endo (East) pucker, and the backbone torsion angles fall into the ac-, ap, sc+, ac+, sc-, and ap ranges (α to ζ for RNA sc-, ap, sc+, sc+, ap, and sc-). The glycosidic torsion angle of apioNA T residues is

approximately -113° (for RNA approximately -160°). A superimposition of trimers 5'-U(apio-T)C-3' and 5'-(dT)UC-3' from strand A in the crystal structures of the apioNA T-modified RNA duplex and the reference duplex [5'-CGAA-(dT)UCG-3']₂, which has a dT rather than the apioNA modification, ⁴⁰ reveals that there is local reorientation of the apiose and 2'-phosphate relative to RNA due to the 3'-2' linkage type of apioNA (Figure 2). The helical rise for the

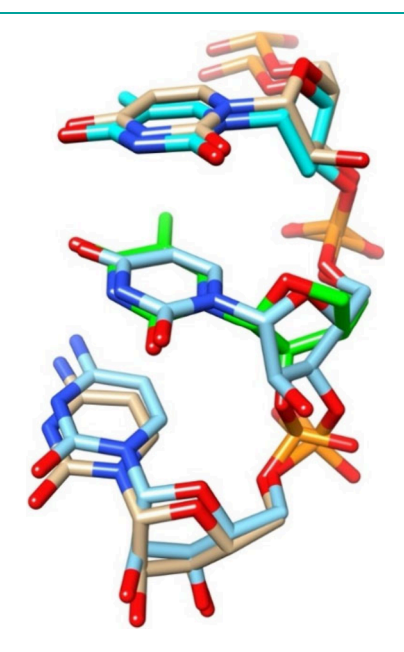


Figure 2. Modification of an RNA with apioNA does not considerably alter the helical structure. Overlay of trimers 5'-U(apio-T)C-3' and 5'-(dT)UC-3' from strand A in the crystal structures of the modified RNA octamer duplexes [5'-(Br⁵C)GAAU(apio-T)CG-3']₂ and [5'-CGAA(dT)UCG-3']₂ (PDB ID 5DEK), respectively. Carbon atoms of apioNA T and dT are highlighted in green and cyan, respectively, and the remaining carbon atoms in the two strands are colored in tan (apioNA T-modified RNA) or light blue (dT-modified RNA).

apioNA T on its 5' side is slightly increased relative to that of RNA, whereas the twists in the two strands are very similar. The difference may contribute to the destabilizing effect of apioNA residues within an RNA duplex. The P(U5)···P(apio-T6) and P(apio-T)···P(C7) distances are 6.1 and 6.0 Å, respectively. The distances between the corresponding phosphorus pairs in the dT-modified RNA reference duplex are both 5.9 Å, demonstrating that an apioNA residue can be accommodated within an RNA backbone without significantly expanding the distance between phosphates.

Modeling of an ApioNA-Modified DNA. To visualize the effects of apioNA on the backbone conformation of DNA, we turned to the crystal structure of the B-DNA Dickerson—Drew dodecamer in complex with RNase H (PDB ID 3D0P).⁴¹ In the crystal, the distance between the 5'- and 3'-phosphate groups of the T at position 7 is 6.75 Å (Figure 3A). Models containing a TNA residue and an apioNA T at this position were built in USCF Chimera and energy-minimized with Amber 14. ApioNA has a 3'-2' connectivity, as does TNA, but contains an additional methylene moiety between the C3' and O3' atoms. In the computational model of the TNA-modified duplex, the phosphate—phosphate distance for the TNA residue is 5.92 Å (Figure 3B), consistent with the shorter backbone of this xeno nucleic acid relative to DNA. In

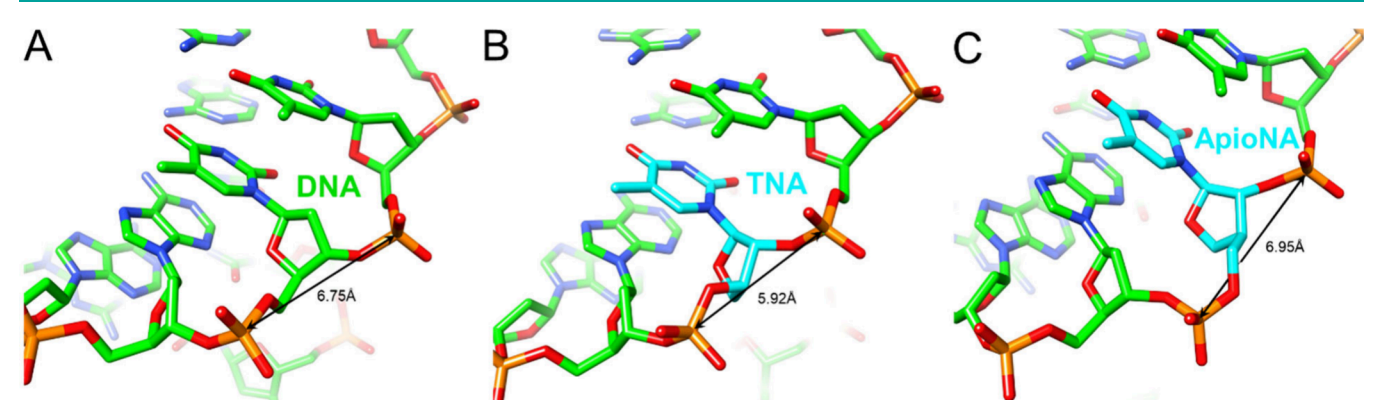


Figure 3. Phosphate—phosphate distances across an apioNA in the context of a DNA duplex are similar to those of native DNA. (A) Central A5—T8 portion of the Dickerson—Drew dodecamer from the crystal in complex with RNase H. (B, C) Computational models of the backbone in duplexes with dT7 replaced with (B) TNA T and (C) apioNA T.

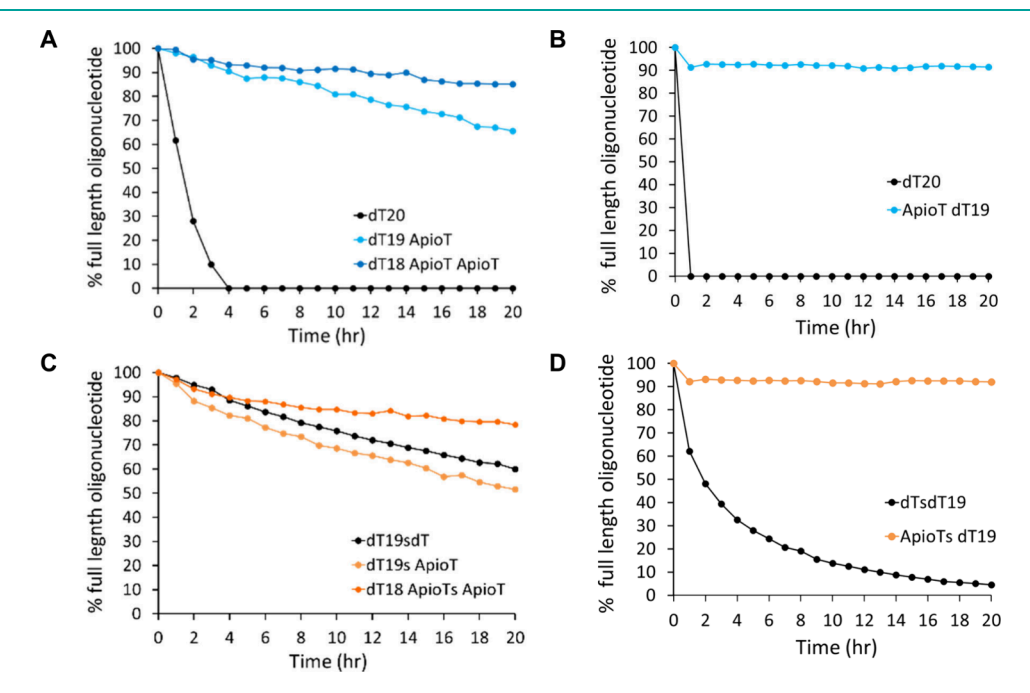


Figure 4. A terminal apioNA residue provides protection from nuclease degradation. (A, B) Percent full-length oligonucleotide remaining for oligonucleotides modified with one or two apioNA residues with phosphodiester linkages at the (A) 3' end (dT19 ApioT and dT18 ApioT ApioT, respectively) and (B) 5' end (ApioTdT19) compared to the control dT20. (C, D) Percent full-length oligonucleotide remaining for oligonucleotides modified with one or two apioNA residues with phosphorothioate linkages at the (C) 3' end (dT19s ApioT and dT18 ApioTs ApioT, respectively) and (D) 5' end (ApioTs dT19) compared to the control dT19sdT. Full-length oligonucleotide was quantified over time in the presence of (A, C) snake venom phosphodiesterase or (B, D) phosphodiesterase II.

the crystal structure of this duplex containing a TNA residue at position 7, the phosphate—phosphate distances for this residue are 5.79 and 6.11 Å (PDB ID 1N1O). The average distance of 5.95 Å in the experimental structure is thus close to that seen in the computational model. By comparison, the phosphate—phosphate distance for apioNA in the modeled duplex is 6.95 Å (Figure 3C). Thus, the backbone is about 1 Å longer compared to TNA and similar to the phosphate—phosphate spacing seen in DNA. The backbone torsion angles for the apioNA residue fall into the sc+, ac-, ap, ac+, sc-, and ac- ranges (α to ζ ; DNA sc-, ap, sc+, ap, ap, and sc-). The pucker of apiose is C4'-exo; this conformation is also adopted by the TNA threose sugar. The

Terminal ApioNA Residues Provide Considerable Protection from Nuclease Degradation. A 20-mer DNA oligonucleotide with one or two apioNA T residues at the 3'

end linked through phosphodiesters was much more stable in the presence of snake venom phosphodiesterase than the control dT_{20} (Figure 4A). More than 70% of the full-length oligonucleotide remained intact after 20 h when one or two modifications were present at the 3′ terminus; in contrast, dT_{20} was completely degraded at this time point. Around 90% of the strand with a single apioNA T at the 5′ end linked through a phosphodiester remained after 20 h in the presence of phosphodiesterase II, whereas the control dT_{20} was completely degraded (Figure 4B). When the terminal apioNA residue or residues were linked through phosphorothioate, the stabilities in the presence of nucleases were similar to those of the all-phosphodiester oligonucleotides with terminal apioNA residues; the dT_{20} controls were considerably stabilized by phosphorothioate modification (Figure 4C,D).

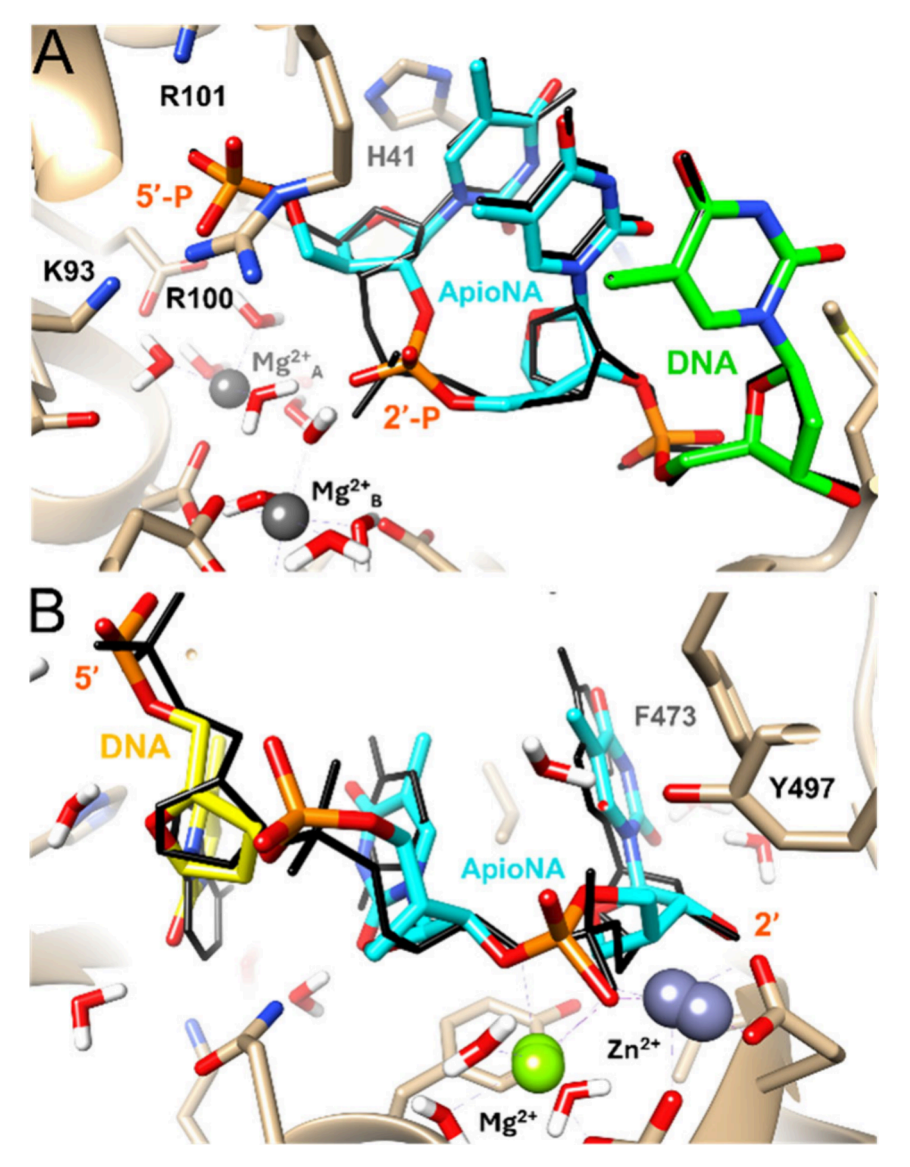


Figure 5. Conformation of an apioNA residue likely interferes with cleavage by nucleases. Computational models of apioNA T-modified trimers in the active sites of (A) the Xrn1 5'-exonuclease and (B) the Klenow fragment 3'-exonuclease based on the crystal structures of the corresponding complexes with DNAs. Carbon atoms of apioNA Ts are colored in cyan, carbon atoms of the 3'-terminal dT in (A) and the 5'-terminal dT in (B) are colored in green and yellow, respectively, and selected residues and divalent metal ions are labeled. Structures of the native DNA oligonucleotides in the crystallographic complexes are overlaid with thin solid black lines.

Modeling of an ApioNA-Modified DNA Explain Improved Nuclease Resistance. We used computational modeling to gain insight into the strong resistance of apioNAmodified oligonucleotides against 5'- and 3'-exonucleases. The crystal structure of Drosophila melanogaster Xrna1 5'exonuclease in complex with 5'-phosphorylated d(T)₃ serves as a model system for human phosphodiesterase II (PDB ID 2Y35).⁴⁵ The Escherichia coli DNA polymerase I Klenow fragment 3'-exonuclease in complex with a short deoxynucleotide serves as model system for snake venom phosphodiesterase (PDB ID 1KFS).46 Two nucleotides at the 5' and 3' ends of the DNA fragments lodged at the 5'-exonuclease and the 3'exonuclease active sites, respectively, were converted into apioNA Ts using UCSF Chimera, 42 and the models were energy-minimized with Amber 14.43 Both active sites have two divalent metal ions. The crystal structure of the Xrn1 complex has only one ion, but we used a starting configuration that contains two Mg²⁺ as previously reported.⁴⁷ These metal ions

do not form direct interactions with a phosphate oxygen, whereas the Mg²⁺ and Zn²⁺ ions in the active site of the Klenow fragment form inner-sphere contacts with a phosphate group. For both the 5'-exonuclease and the 3'-exonuclease, incorporation of apioNA Ts resulted in considerable changes in the position and orientation of the phosphate groups that are processed (Figure 5A,B). At the Klenow fragment 3'-exonuclease active site, the presence of the apioNA T dimer at the 3' end of the oligonucleotide also triggered shifts of the two metal ions in the modeled complex relative to their positions in the crystal structure with DNA (Figure 5B). These conformational differences likely underlie the excellent protection against exonuclease degradation afforded by the apioNA modification.

TNA Polymerase Recognition of Apio-NA NTPs. For use as therapeutics or diagnostic tools, aptamers must be stable in a biological milieu. TNA polymerases have been engineered that allow isolation of functional TNA aptamers.²⁸ Given the

A
5'-d-GTCCCCTTGGGGATACCACC
3'-d-CAGGGGAACCCCTATGGTGGTTGAAATAATTCACACACAAATCGCTATCCTCCCACAGGG-5'

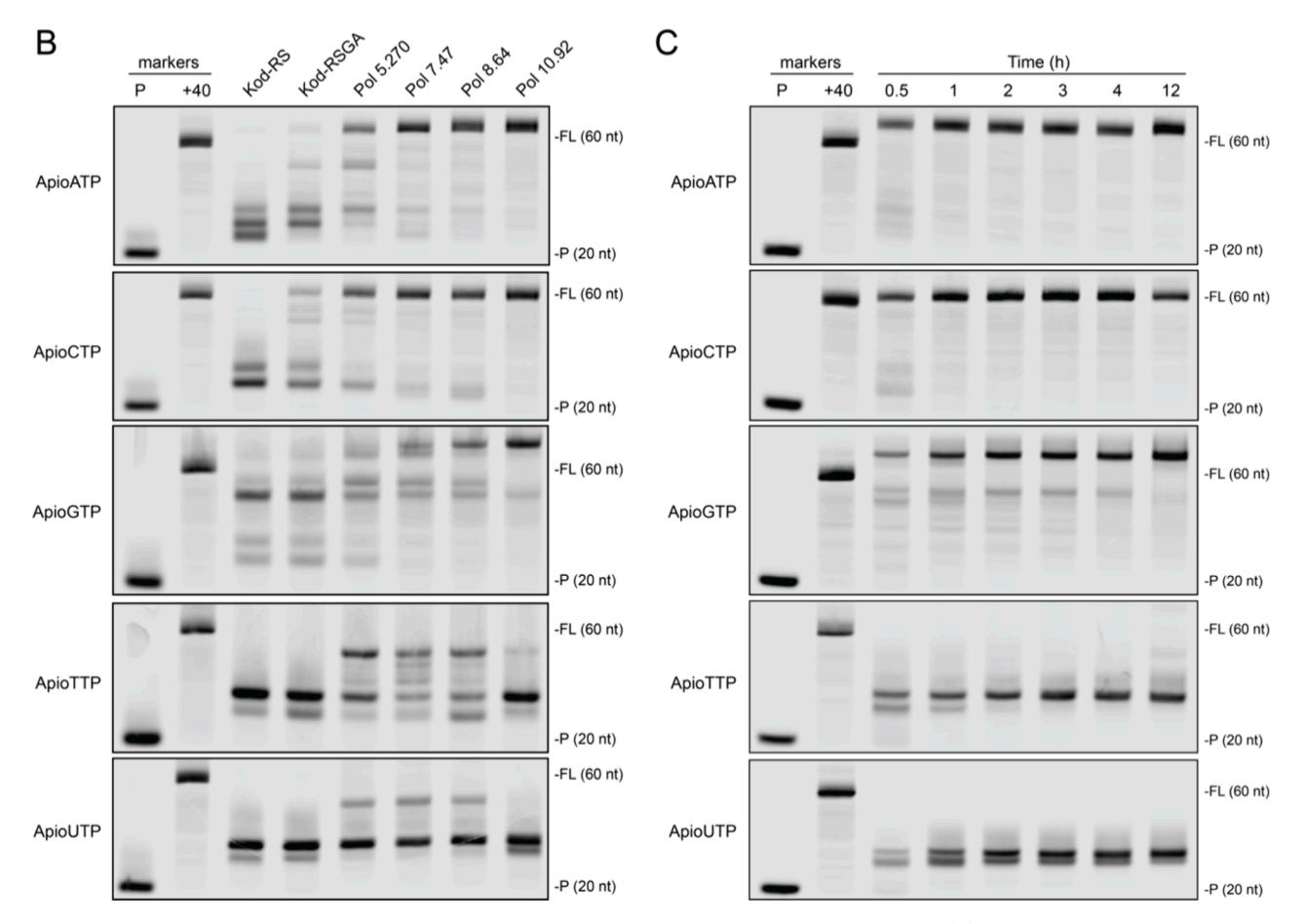


Figure 6. TNA polymerases use some apioNA NTPs as substrates in TNA primer extension reactions. (A) Polyacrylamide gel analysis of 12 h extension reactions with indicated TNA polymerases in the presence of indicated apioNA NTP. (B) Analysis of primer extension as a function of time using the 10-92 TNA polymerase. P indicates the primer, and +40 corresponds to complete extension of the primer with TNA. Reactions were performed by individually replacing each TNA NTP substrate with the corresponding apioNA NTP.

close structural similarity between TNA and apioNA, we evaluated whether polymerases engineered to efficiently use TNA NTPs would recognize apioNA NTPs as substrates. The 5'-IR680-labeled DNA primer was annealed to a DNA template (Figure 6A), and samples containing mixtures of TNA triphosphates with each nucleotide individually replaced with its corresponding apioNA NTP were prepared. Following a 12 h incubation at 55 °C, product formation was visualized by 10% denaturing polyacrylamide gel electrophoresis. Polymerases 5-270, 7-47, 8-64, and 10-92 used apioNA NTPs as substrates 48 (Figure 6B). Only apioNA ATP, apioNA CTP, and apioNA GTP served as substrates. By comparison, poor extension efficiency was observed in the presence of apioNA TTP and apioNA UTP, possibly due to misalignment of the substrate in the active site. Additionally, the first insertion site for apio T/U requires three sequential insertions, which may be difficult due to stacking or other geometric requirements in the active site. Among the polymerases tested, 10-92 most efficiently recognized apioNA NTPs. For example, more full-length product formation was observed in the presence of apioNA GTP with this polymerase than in reactions with polymerase 5-270, 7-47, or 8-64. Time-course analyses of the reactions catalyzed by 10-92 revealed that fulllength product was observed in as little as 30 min in individual reactions containing apioNA ATP, apioNA CTP, or apioNA GTP. Taken together, these results suggest that 10-92 could be an ideal starting point for evolving a bona fide apioNA polymerase.

CONCLUSIONS

Synthesis of T, C, A, and G apioNA phosphoramidites and incorporation into oligonucleotide sequences were reported recently in the patent literature. These routes do not maintain the stereopurity of the pentose sugar in the starting material or rely on multistep homologation. Here we report a route starting from the naturally occurring sugar D-(+)-xylose. Suitable reaction conditions and the choice of solvent gave exclusively β -glycosylated nucleosides. We synthesized apioNA building blocks bearing A, U, G, C, T, and 5-meC as phosphoramidites, H-phosphonates, solid supports, and nucleotide triphosphates.

The apioNA residues thermally destabilized RNA and DNA duplexes, and the observed destabilization is similar to what is observed for TNA. Further, although a self-complementary apioNA oligomer does form a duplex, the dodecamer tested was considerably less stable than the DNA duplex of the same

sequence. The crystal structure of the apioNA-modified RNA octamer showed that the apioNA residue adopts an RNA-like structure, but local reorientation of the apioNA sugar and 2′-phosphate and the difference in helical rise on the 5′ side of the apioNA T relative to RNA may contribute to the destabilizing effect of apioNA residues within an RNA duplex. Importantly, the apioNA residue can be accommodated within an RNA backbone without significantly expanding the distance between phosphates. Molecular modeling revealed that in the context of a DNA duplex, the phosphate—phosphate distance for the apioNA is similar to that of DNA. In contrast, the phosphate—phosphate distance across a TNA is about 1 Å shorter.

Terminal modification of a DNA oligonucleotide with apioNA improved resistance to both 3′- and 5′-exonucleases compared to that of a fully DNA oligonucleotide. A phosphorothioate linkage was not necessary for this stabilization. Molecular modeling of the active sites of 5′- and 3′-exonucleases indicated that incorporation of apioNA Ts at the termini of the DNA substrate results in considerable changes in the position and orientation of the phosphate groups, presumably impairing enzymatic cleavage.

We evaluated the apioNA NTPs for their ability to serve as substrates in TNA-dependent polymerase reactions. The A, C, and G apioNA NTPs were polymerase substrates, and 10-92 polymerase very efficiently polymerized these NTPs. These apioNA NTPs could be used to develop novel aptamer structures. These analogs were previously shown to have antiviral potential. Whether the apioNAs are substrates for human polymerases is relevant to therapeutic applications and should be explored.

The utility of apioNAs in therapeutic oligonucleotides warrants an evaluation. The very high nuclease resistance even as a phosphodiester will be an advantage in therapeutics based on nucleic acids. Although these residues destabilize duplex formation, this can be an asset. For example, strategic placement could facilitate release of the therapeutic strand in antisense technology. 49,50 Previous work has shown that modifications such as glycol nucleic acids and TNA in the seed region of the siRNA antisense strand mitigate off-target effects. Use of apioNAs for RNase H-based antisense therapeutics would allow reduction of phosphorothioate content and reduction of undesirable protein binding, which is a safety advantage. 50,51 For siRNAs, the diastereomeric isomer mixture will be reduced when apioNA is used at the termini without compromising the metabolic stability. In summary, the synthetic routes to apioNA building blocks described here will make it possible to evaluate these modifications in various nucleic acid-based therapeutic modalities. Experiments testing these modifications in siRNAs are underway, and results will be reported in due course. Since the submission of this manuscript, apioNA and extended apioNA analogs have been evaluated by Mei et al.⁶⁰ as 3' modifications for nuclease resistance, exhibiting results similar to reported here. Furthermore, structural modeling studies of favorable interactions of these analogs at the 3'-overhang positions of siRNA have been shown in the context of PAZ domain of the argonaute 2 enzyme. These observations underscore the results reported in the present study.

METHODS

Syntheses and Compound Characterizations. Synthetic procedures and characterizations of all new compounds and oligonucleotides are reported in the Supporting Information.

Melting Temperature Analyses. For $T_{\rm m}$ determination, samples were prepared at a concentration of 2 μ M for each strand in 1× PBS (pH 7.4). $T_{\rm m}$ values were obtained from the maxima of the first derivatives of the averages of two heating and two cooling curves (A_{260} vs temperature) recorded in 1× PBS buffer (pH 7.4) using a 2.0 μ M concentration of each strand. $\Delta T_{\rm m}$ was calculated based on the difference between the $T_{\rm m}$ of the duplex with apioNA residues and the parent RNA/RNA, DNA/DNA, or RNA/DNA duplex.

Nuclease Resistance Assays. Oligonucleotides were prepared at final concentrations of 0.1 mg mL⁻¹ in 50 mM Tris (pH 7.2) and 10 mM MgCl₂ for assays in the presence of 150 mU/mL 3'-specific snake venom phosphodiesterase or in 50 mM sodium acetate (pH 6.5) and 10 mM MgCl₂ for assays in the presence of 500 mU/mL 5'specific exonuclease phosphodiesterase II. The exonuclease was added to the oligonucleotide solution immediately prior to the first injection onto the HPLC column, and the full-length strand was quantified over a 24 h period at 25 °C. Samples were analyzed on a Dionex DNAPac PA200 analytical column at 30 °C. The gradient was from 37% to 52% 1 M NaBr, 10% acetonitrile (ACN), and 20 mM sodium phosphate buffer (pH 11) over 10 min at a flow rate of 1 mL/min with absorbance monitored at 260 nm. Percent full-length oligonucleotide was calculated by dividing the area under the curve of the peak corresponding to full-length oligonucleotide at a given time point by that at the first time point and multiplying by 100. The half-life was determined by fitting to first-order kinetics. Each degradation experiment was performed in duplicate.

ApioNA NTP Polymerization Assay. Engineered TNA polymerases (Kod-RS, Kod-RSGA, Pol 5-270, Pol 7-47, Pol 8-64, and Pol 10-92) were evaluated for their recognition of apioNA NTPs as substrates in a mixture of TNA NTPs in which each individual TNA NTP was replaced with its corresponding apioNA NTP. Each primer extension reaction was performed in 20 μ L reaction volumes containing 0.5 μ M 5'-IR800 PBS8 primer, 0.7 μ M DNA template, 1× ThermoPol Buffer (20 mM Tris-HCl (pH 8.8), 10 mM KCl, 10 mM (NH₄)₂SO₄, 20 mM MgSO₄), 100 μ M NTP mixture, and 0.5 μ M TNA polymerase. The primer was annealed to the template in 1× ThermoPol buffer at 90 °C for 5 min and immediately placed on ice for 5 min, followed by the addition of NTPs and enzymes to initiate the reaction. The reaction mixtures were placed in a thermal cycler at 55 °C, and the reactions were monitored over 12 h. At each time point, 1 μ L of the reaction mixture was removed, mixed with 39 μ L of quenching buffer (95% formamide, 25 mM EDTA, pH 8.0), and denatured at 95 °C for 10 min. Aliquots of 10 μL were loaded onto a 10% urea polyacrylamide gel, run at 16 W for 1.5 h, and imaged using a Li-Cor Odyssey CLx imager.

Crystallization, Data Collection, Model Building, and Refinement. Crystals of r[(5BrC)GAAU(apio-T)CG] were grown by sitting-drop vapor diffusion. The drops contained 400 nL of 1 mM RNA and 400 nL of buffer containing 10% 2-methyl-2,4-pentandiol (MPD), 12 mM spermine·4HCl, 80 mM KCl, and 40 mM sodium cacodylate (pH 7.0). Drops were equilibrated against 70 mL of 40% MPD. Crystals were harvested directly from drops using Mitegen microloops and flash-cooled by plunging into liquid nitrogen. Data collection was performed remotely at the BioMAX beamline at the MAX IV synchrotron light source in Sweden. The diffraction data were collected at 0.9184 Å wavelength for bromine-SAD data and processed on-site using EDNA2 front end to XDS. Diffraction data were phased using the HKL2MAPS interface to SHELXC, SHELXC, SHELXD, SALELXE, SALELXE, Model building was done using Autobuild And manually using COOT. Refinement was done using PHENIX. Data collection and refinement statistics are presented in Table S8.

ASSOCIATED CONTENT

Supporting Information

The Supporting Information is available free of charge at https://pubs.acs.org/doi/10.1021/acschembio.5c00591.

2D NOESY spectra of apioNA nucleosides, oligonucleotide sequences and mass spectroscopy data, melting

temperatures of duplexes containing strands modified with apioNA, and synthetic procedures and NMR characterizations of all novel compounds (PDF)

AUTHOR INFORMATION

Corresponding Author

Muthiah Manoharan – Alnylam Pharmaceuticals, Cambridge, Massachusetts 02142, United States; oorcid.org/0000-0002-7931-1172; Email: mmanoharan@alnylam.com

Authors

- Victorio Jauregui-Matos Alnylam Pharmaceuticals, Cambridge, Massachusetts 02142, United States; Summer Intern 2024, Drug Innovation Group, Alnylam Pharmaceuticals, Cambridge, Massachusetts 02142, United States; o orcid.org/0000-0003-2009-5521
- Dhrubajyoti Datta Alnylam Pharmaceuticals, Cambridge, Massachusetts 02142, United States; o orcid.org/0000-0003-2077-1294
- Jayanta Kundu Alnylam Pharmaceuticals, Cambridge, Massachusetts 02142, United States
- **Vathan Kumar** Alnylam Pharmaceuticals, Cambridge, Massachusetts 02142, United States; o orcid.org/0000-0002-2837-419X
- Joel M. Harp Department of Biochemistry, Vanderbilt University School of Medicine, Nashville, Tennessee 37232, United States
- Adekunle Adebayo Alnylam Pharmaceuticals, Cambridge, Massachusetts 02142, United States
- Daniel Donnelly Alnylam Pharmaceuticals, Cambridge, Massachusetts 02142, United States
- Esau Medina Department of Pharmaceutical Sciences, University of California, Irvine, California 92697-3958, United States
- John C. Chaput Department of Pharmaceutical Sciences, University of California, Irvine, California 92697-3958, *United States;* orcid.org/0000-0003-1393-135X
- Martin Egli Department of Biochemistry, Vanderbilt University School of Medicine, Nashville, Tennessee 37232, *United States*; orcid.org/0000-0003-4145-356X

Complete contact information is available at: https://pubs.acs.org/10.1021/acschembio.5c00591

Notes

The authors declare no competing financial interest.

REFERENCES

- (1) Pičmanová, M.; Møller, B. L. Apiose: one of nature's witty games. Glycobiology 2016, 26 (5), 430-442.
- (2) Carter, M. S.; Zhang, X.; Huang, H.; Bouvier, J. T.; Francisco, B. S.; Vetting, M. W.; Al-Obaidi, N.; Bonanno, J. B.; Ghosh, A.; Zallot, R. G.; et al. Functional assignment of multiple catabolic pathways for dapiose. Nat. Chem. Biol. 2018, 14 (7), 696-705.
- (3) Parikh, D. K.; Watson, R. R. Synthesis of branched-chain apiosylpyrimidines and their inhibition of lymphocyte proliferation. J. Med. Chem. 1978, 21 (7), 706-709.
- (4) Kis, P.; Horváthová, E.; Gálová, E.; Ševčovičová, A.; Antalová, V.; Karnišová Potocká, E.; Mastihuba, V.; Mastihubová, M. Synthesis of Tyrosol and Hydroxytyrosol Glycofuranosides and Their Biochemical and Biological Activities in Cell-Free and Cellular Assays. Molecules 2021, 26 (24), No. 7607.
- (5) Toti, K. S.; Derudas, M.; Pertusati, F.; Sinnaeve, D.; Van den Broeck, F.; Margamuljana, L.; Martins, J. C.; Herdewijn, P.; Balzarini, J.; McGuigan, C.; et al. Synthesis of an Apionucleoside Family and

- Discovery of a Prodrug with Anti-HIV Activity. J. Org. Chem. 2014, 79 (11), 5097-5112.
- (6) Jung, M. E.; Toyota, A. Efficient synthesis of several methyleneexpanded oxetanocin nucleoside analogues. Tetrahedron Lett. 2000, 41 (19), 3577-3581.
- (7) Panda, A.; Satpati, S.; Dixit, A.; Pal, S. Novel homologated-apio adenosine derivatives as A3 adenosine receptor agonists: design, synthesis and molecular docking studies. RSC Adv. 2016, 6 (14), 11233-11239.
- (8) Panda, A.; Islam, S.; Santra, M. K.; Pal, S. Lead tetraacetate mediated one pot oxidative cleavage and acetylation reaction: an approach to apio and homologated apio pyrimidine nucleosides and their anticancer activity. RSC Adv. 2015, 5 (100), 82450-82459.
- (9) Sivakrishna, B.; Islam, S.; Santra, M. K.; Pal, S. Synthesis and cytotoxic evaluation of apioarabinofuranosyl pyrimidines. Drug Dev. Res. 2020, 81 (3), 274-282.
- (10) Sivakrishna, B.; Shukla, M.; Santra, M. K.; Pal, S. Design, synthesis and cytotoxic evaluation of truncated 3'-deoxy- 3',3'difluororibofuranosyl pyrimidine nucleosides. Carbohydr. Res. 2020, 497, No. 108113.
- (11) Jin, D. Z.; Kwon, S. H.; Moon, H. R.; Gunaga, P.; Kim, H. O.; Kim, D.-K.; Chun, M. W.; Jeong, L. S. Synthesis of D- and L-apio nucleoside analogues with 2'-hydroxyl group as potential anti-HIV agents. Bioorg. Med. Chem. 2004, 12 (5), 1101-1109.
- (12) Hammerschmidt, F.; Öhler, E.; Polsterer, J.-P.; Zbiral, E.; Balzarini, J.; Declercq, E. Ein einfacher Weg zu 3'-Desoxy- α -L- und 3'-Desoxy- β -D-apionucleosiden. Liebigs Ann. 1995, 1995 (3), 559–565.
- (13) Reist, E. J.; Calkins, D. F.; Goodman, L. Branched chain sugars. The synthesis of adenine nucleosides of 3- deoxy-3-C-hydroxymethyl-D-erythrofuranose and 2-deoxy-2-C-hydroxymethyl-D-erythrofuranose. J. Am. Chem. Soc. 1968, 90 (14), 3852-3857.
- (14) Doboszewski, B.; Herdewijn, P. Branched-chain nucleosides: Synthesis of 3'-deoxy-3'-C-hydroxymethyl- α -L-lyxopyranosyl thymine and 3'-deoxy-3'-C-hydroxymethyl-α-L-threofuranosyl thymine. Tetrahedron 1996, 52 (5), 1651-1668.
- (15) Kataoka, M.; Sato, K.; Matsuda, A. Synthesis of 3'deoxyapionucleoside triphosphates and their incorporation into DNA by DNA polymerase. Nucleic Acids Symp. Ser. 2008, 52 (1), 281 - 282.
- (16) Kataoka, M.; Kouda, Y.; Sato, K.; Minakawa, N.; Matsuda, A. Highly efficient enzymatic synthesis of 3'-deoxyapionucleic acid (apioNA) having the four natural nucleobases. Chem. Commun. 2011, 47 (30), 8700-8702.
- (17) Toti, K.; Renders, M.; Groaz, E.; Herdewijn, P.; Van Calenbergh, S. Nucleosides with Transposed Base or 4'-Hydroxymethyl Moieties and Their Corresponding Oligonucleotides. Chem. Rev. 2015, 115 (24), 13484-13525.
- (18) Culbertson, M. C.; Temburnikar, K. W.; Sau, S. P.; Liao, J.-Y.; Bala, S.; Chaput, J. C. Evaluating TNA stability under simulated physiological conditions. Bioorg. Med. Chem. Lett. 2016, 26 (10), 2418-2421.
- (19) Lee, E. M.; Setterholm, N. A.; Hajjar, M.; Barpuzary, B.; Chaput, J. C. Stability and mechanism of threose nucleic acid toward acid-mediated degradation. Nucleic Acids Res. 2023, 51 (18), 9542-
- (20) Schöning, K. U.; Scholz, P.; Guntha, S.; Wu, X.; Krishnamurthy, R.; Eschenmoser, A. Chemical Etiology of Nucleic Acid Structure: The α -Threofuranosyl- $(3' \rightarrow 2')$ Oligonucleotide System. Science 2000, 290 (5495), 1347-1351.
- (21) Matsuda, S.; Bala, S.; Liao, J. Y.; Datta, D.; Mikami, A.; Woods, L.; Harp, J. M.; Gilbert, J. A.; Bisbe, A.; Manoharan, R. M.; et al. Shorter Is Better: The alpha-(1)-Threofuranosyl Nucleic Acid Modification Improves Stability, Potency, Safety, and Ago2 Binding and Mitigates Off-Target Effects of Small Interfering RNAs. J. Am. Chem. Soc. 2023, 145 (36), 19691-19706.
- (22) Wang, F.; Liu, L. S.; Li, P.; Lau, C. H.; Leung, H. M.; Chin, Y. R.; Tin, C.; Lo, P. K. Cellular uptake, tissue penetration, biodistribution, and biosafety of threose nucleic acids: Assessing in vitro and in vivo delivery. Mater. Today Bio 2022, 15, No. 100299.

ı

https://doi.org/10.1021/acschembio.5c00591 ACS Chem. Biol. XXXX, XXX, XXX—XXX

- (23) Nguyen, K.; Wang, Y.; England, W. E.; Chaput, J. C.; Spitale, R. C. Allele-Specific RNA Knockdown with a Biologically Stable and Catalytically Efficient XNAzyme. *J. Am. Chem. Soc.* **2021**, *143* (12), 4519–4523.
- (24) Wang, Y.; Nguyen, K.; Spitale, R. C.; Chaput, J. C. A biologically stable DNAzyme that efficiently silences gene expression in cells. *Nat. Chem.* **2021**, *13* (4), 319–326.
- (25) Wang, F.; Liu, L. S.; Lau, C. H.; Han Chang, T. J.; Tam, D. Y.; Leung, H. M.; Tin, C.; Lo, P. K. Synthetic α -l-Threose Nucleic Acids Targeting BcL-2 Show Gene Silencing and in Vivo Antitumor Activity for Cancer Therapy. ACS Appl. Mater. Interfaces **2019**, 11 (42), 38510–38518.
- (26) Liu, L. S.; Leung, H. M.; Tam, D. Y.; Lo, T. W.; Wong, S. W.; Lo, P. K. α -L-Threose Nucleic Acids as Biocompatible Antisense Oligonucleotides for Suppressing Gene Expression in Living Cells. ACS Appl. Mater. Interfaces 2018, 10 (11), 9736–9743.
- (27) Chaput, J. C.; Egli, M.; Herdewijn, P. The XNA alphabet. *Nucleic Acids Res.* **2025**, 53 (13), No. gkaf635.
- (28) Dunn, M. R.; McCloskey, C. M.; Buckley, P.; Rhea, K.; Chaput, J. C. Generating Biologically Stable TNA Aptamers that Function with High Affinity and Thermal Stability. *J. Am. Chem. Soc.* **2020**, *142* (17), 7721–7724.
- (29) Nikoomanzar, A.; Chim, N.; Yik, E. J.; Chaput, J. C. Engineering polymerases for applications in synthetic biology. *Q. Rev. Biophys.* **2020**, *53*, No. e8.
- (30) Datta, D.; Theile, C. S.; Wassarman, K.; Qin, J.; Racie, T.; Schmidt, K.; Jiang, Y.; Sigel, R.; Janas, M. M.; Egli, M.; et al. Rational optimization of siRNA to ensure strand bias in the interaction with the RNA-induced silencing complex. *Chem. Commun.* **2023**, *59* (42), 6347–6350.
- (31) Yamada, K.; Hariharan, V. N.; Caiazzi, J.; Miller, R.; Ferguson, C. M.; Sapp, E.; Fakih, H. H.; Tang, Q.; Yamada, N.; Furgal, R. C.; et al. Enhancing siRNA efficacy in vivo with extended nucleic acid backbones. *Nat. Biotechnol.* **2025**, 43 (6), 904–913.
- (32) Datta, D.; Kundu, J.; Miller, P.; Khan, M. S.; Salinas, J.; Qin, J.; LeBlanc, S.; Nguyen, T.; Peng, H.; Theile, C. S.; et al. Expanding the binding space of argonaute-2: incorporation of either *E* or *Z* isomers of 6'-vinylphosphonate at the 5' end of the antisense strand improves RNAi activity. *Chem. Commun.* **2025**, *61* (36), 6659–6662.
- (33) Mei, H.; Xiong, C.; Wen, J.; He, L.; Zhao, Y. Sugar ring modified nucleoside phosphoramidite monomer, preparation method and use. WO 2024139896, 2024.
- (34) Beigelman, L.; Rajwanshi, V. K.; Hossbach, M.; Pandey, R. K.; Hong, J.; Eltepu, L.; Montero, S. M.; De Costa, N. T. S. Modified short interfering nucleic acid (siNA) molecules and uses for disease treatment. WO 2023039005, 2023.
- (35) Ahmad, N.; Zakaria, M. R. Chapter 8 Oligosaccharide from Hemicellulose. In *Lignocellulose for Future Bioeconomy*, Ariffin, H., Sapuan, S. M., Hassan, M. A., Eds.; Elsevier, 2019; pp 135–152.
- (36) Vorbrüggen, H.; Bennua, B. Nucleoside syntheses, XXV1. A new simplified nucleoside synthesis. *Chem. Ber.* **1981**, *114*, 1279–1286
- (37) Choi, W. B.; Wilson, L. J.; Yeola, S.; Liotta, D. C.; Schinazi, R. F. In situ complexation directs the stereochemistry of N-glycosylation in the synthesis of thialanyl and dioxolanyl nucleoside analogs. *J. Am. Chem. Soc.* **1991**, *113* (24), 9377–9379.
- (38) Zlatev, I.; Manoharan, M.; Vasseur, J.-J.; Morvan, F. Solid-Phase Chemical Synthesis of 5'-Triphosphate DNA, RNA, and Chemically Modified Oligonucleotides. *Curr. Protoc. Nucleic Acid Chem.* **2012**, *50* (1), 1.28.21–21.28.16.
- (39) Kataoka, M.; Kouda, Y.; Sato, K.; Minakawa, N.; Matsuda, A. Highly efficient enzymatic synthesis of 3'-deoxyapionucleic acid (apioNA) having the four natural nucleobases. *Chem. Commun.* **2011**, 47 (30), 8700–8702.
- (40) Kel'in, A. V.; Zlatev, I.; Harp, J.; Jayaraman, M.; Bisbe, A.; O'Shea, J.; Taneja, N.; Manoharan, R. M.; Khan, S.; Charisse, K.; et al. Structural Basis of Duplex Thermodynamic Stability and Enhanced Nuclease Resistance of 5'-C-Methyl Pyrimidine-Modified Oligonucleotides. J. Org. Chem. 2016, 81 (6), 2261–2279.

- (41) Pallan, P. S.; Egli, M. Insights into RNA/DNA hybrid recognition and processing by RNase H from the crystal structure of a non-specific enzyme-dsDNA complex. *Cell Cycle* **2008**, *7* (16), 2562–2569.
- (42) Pettersen, E. F.; Goddard, T. D.; Huang, C. C.; Couch, G. S.; Greenblatt, D. M.; Meng, E. C.; Ferrin, T. E. UCSF Chimera—a visualization system for exploratory research and analysis. *J. Comput. Chem.* **2004**, 25 (13), 1605–1612.
- (43) Case, D. A.; Cheatham, T. E., III; Darden, T.; Gohlke, H.; Luo, R.; Merz, K. M., Jr.; Onufriev, A.; Simmerling, C.; Wang, B.; Woods, R. J. The Amber biomolecular simulation programs. *J. Comput. Chem.* **2005**, *26* (16), 1668–1688.
- (44) Wilds, C. J.; Wawrzak, Z.; Krishnamurthy, R.; Eschenmoser, A.; Egli, M. Crystal structure of a B-form DNA duplex containing (L)- α -threofuranosyl (3' \rightarrow 2') nucleosides: a four-carbon sugar is easily accommodated into the backbone of DNA. *J. Am. Chem. Soc.* **2002**, 124 (46), 13716–13721.
- (45) Jinek, M.; Coyle, S. M.; Doudna, J. A. Coupled 5' nucleotide recognition and processivity in Xrn1-mediated mRNA decay. *Mol. Cell* **2011**, *41* (5), 600–608.
- (46) Brautigam, C. A.; Steitz, T. A. Structural principles for the inhibition of the 3'-5' exonuclease activity of *Escherichia coli* DNA polymerase I by phosphorothioates. *J. Mol. Biol.* **1998**, 277 (2), 363–377.
- (47) Datta, D.; Kumar, P.; Kundu, J.; Qin, J.; Gilbert, J. A.; Schofield, S.; Donnelly, D. P.; Liu, J.; Degaonkar, R.; Egli, M.; et al. Improved In Vivo Metabolic Stability and Silencing Efficacy of siRNAs with Phosphorothioate Linkage-Free, GalNAc-Conjugated Sense Strands Containing Morpholino-LNA Modifications. *Org. Lett.* **2024**, *26* (47), 10061–10065.
- (48) Maola, V. A.; Yik, E. J.; Hajjar, M.; Lee, J. J.; Holguin, M. J.; Quijano, R. N.; Nguyen, K. K.; Ho, K. L.; Medina, J. V.; Chim, N.; et al. Directed evolution of a highly efficient TNA polymerase achieved by homologous recombination. *Nat. Catal.* **2024**, *7* (11), 1173–1185.
- (49) Crooke, S. T.; Seth, P. P.; Vickers, T. A.; Liang, X. H. The Interaction of Phosphorothioate-Containing RNA Targeted Drugs with Proteins Is a Critical Determinant of the Therapeutic Effects of These Agents. J. Am. Chem. Soc. 2020, 142 (35), 14754–14771.
- (50) Egli, M.; Manoharan, M. Chemistry, structure and function of approved oligonucleotide therapeutics. *Nucleic Acids Res.* **2023**, *51* (6), 2529–2573.
- (51) Crooke, S. T.; Vickers, T. A.; Liang, X. H. Phosphorothioate modified oligonucleotide-protein interactions. *Nucleic Acids Res.* **2020**, 48 (10), 5235–5253.
- (52) Kabsch, W. XDS. Acta Crystallogr., Sect. D: Biol. Crystallogr. **2010**, 66 (2), 125–132.
- (53) Pape, T.; Schneider, T. R. HKL2MAP: a graphical user interface for macromolecular phasing with SHELX programs. *J. Appl. Crystallogr.* **2004**, 37 (5), 843–844.
- (54) Sheldrick, G. SHELXC; Göttingen University: Göttingen, Germany, 2003.
- (55) Schneider, T. R.; Sheldrick, G. M. Substructure solution with SHELXD. *Acta Crystallogr., Sect. D: Biol. Crystallogr.* **2002**, 58 (10), 1772–1779.
- (56) Sheldrick, G. M. Macromolecular phasing with SHELXE. Z. Kristallogr. 2002, 217 (12), 644–650.
- (57) Afonine, P. V.; Grosse-Kunstleve, R. W.; Echols, N.; Headd, J. J.; Moriarty, N. W.; Mustyakimov, M.; Terwilliger, T. C.; Urzhumtsev, A.; Zwart, P. H.; Adams, P. D. Towards automated crystallographic structure refinement with phenix.refine. *Acta Crystallogr., Sect. D: Biol. Crystallogr.* **2012**, *68* (4), 352–367.
- (58) Emsley, P.; Lohkamp, B.; Scott, W. G.; Cowtan, K. Features and development of Coot. *Acta Crystallogr., Sect. D: Biol. Crystallogr.* **2010**. *66* (4), 486–501.
- (59) Liebschner, D.; Afonine, P. V.; Baker, M. L.; Bunkóczi, G.; Chen, V. B.; Croll, T. I.; Hintze, B.; Hung, L. W.; Jain, S.; McCoy, A. J.; et al. Macromolecular structure determination using X-rays,

neutrons and electrons: recent developments in Phenix. *Acta Crystallogr., Sect. D: Struct. Biol.* **2019**, *75* (10), 861–877. (60) Gao, Y.; Xiong, C.; Zhang, C.; Wen, J.; Chen, X.; Li, X.; Dai, Z.; Zhou, L.; Mei, H. 3'-C-Extended TNA: De Novo Synthesis, Enhanced Exonuclease Resistance, and Functional siRNA 3'-Overhang Modifications Without Compromising Gene Silencing. *Chem. Eur. J.* **2025**, *31*, No. e02182.



CAS BIOFINDER DISCOVERY PLATFORM™

BRIDGE BIOLOGY AND CHEMISTRY FOR FASTER ANSWERS

Analyze target relationships, compound effects, and disease pathways

Explore the platform

